Directly modulated DFB lasers on InP membrane on Si

A. Zozulia[a], G. Nazarikov[a], R. Schatz[b], S. Rihani[c], G. Berry[c], K. A. Williams[a], and Y. Jiao[a]

[a]Eindhoven Hendrik Casimir Institute (EHCI), Eindhoven University of Technology, 5600MB Eindhoven, The Netherlands
[b]KTH Royal Institute of Technology, Applied Physics, Photonics, Stockholm, Sweden
[c]Huawei Technologies Research & Development (UK) Ltd, IP5 3RE Ipswich, UK
e-mail: a.zozulia@tue.nl

Abstract

We designed, fabricated and measured DFB lasers on InP on Si (IMOS) photonic integration platform. The layer stack was optimized to achieve a higher relaxation oscillation frequency compared to previous generation of IMOS lasers. We measured static and dynamic characteristics of a 250 μm DFB laser, which shows up to 600 μW power in the fiber and 3dB bandwidth up to 15 GHz. We also performed a data transmission experiment and achieved open eye diagrams at 25 Gbit/s.

Introduction

The amount of data produced, stored and transferred world-wide over optical networks grows every year. In the field of short-reach datacom telecommunication there is a strong demand for efficient and small footprint optoelectronic transceivers. Directly modulated lasers (DMLs) gained a significant attention from the industry, since they can provide high data rates at low operating power for short-distance communication (up to 2 km). A huge progress has been made in performance of DMLs over the last few years. For O-band, lasers based on InGaAlAs multiple quantum wells (MQW) demonstrated a bandwidth of 108 GHz at room temperature [1] and up to 74 GHz at 85 °C [2]. In C-band, DMLs with bandwidth >67 GHz were reported [3]. However, there is still a need to integrate high-speed DML into complex optoelectronic systems, in particular, the 3D integration with electronics is desired, as it can significantly increase the bandwidth of electronic connections to the laser and reduce the overall power consumption of the transceiver [4]. InP membrane on Si (IMOS) platform has this potential. In IMOS, InGaAsP based semiconductor optical amplifiers (SOAs) are monolithically integrated with highly confined sub-micron passive waveguides in a 1 μm thin photonic membrane, adhesively bonded to a Si substrate [5]. The platform offers a broad range of active and passive building blocks, including DFB and DBR lasers, photonic crystal reflector (PhC) lasers, multimode interference splitters (MMI), polarization converters and many others, allowing photonic integrated circuits (PIC) designers to design highly functional systems. The adhesive bonding used in IMOS opens the possibility of integration with CMOS or InP-based electronics on the substrate [6]. In this work, we explored the performance of DFB lasers on IMOS for direct modulation. We optimized the previously reported IMOS layer stack and process flow to increase the DML bandwidth, fabricated and measured static and dynamic characteristics of DFB lasers. Finally, we made an analysis of measured data and gave conclusions about the further improvement of DML performance.

Laser design

A DM bandwidth of a semiconductor laser is limited by 3 main factors: relaxation oscillation frequency (ω_r), damping (γ) and RC constant ω_p [7], [8]. To increase ω_r, we

increased the number of QW from 4 to 8 and reduced the thickness of the InGaAsP core to 300 nm. To reduce the device foot-print, we designed a low-reflection butt-joint interface to the passive InGaAsP waveguide, fabricated by epitaxial regrowth [9]. The schematic cross-section of the laser is shown on Figure 1a, and the FIB cut made after the fabrication is on the Figure 1b. IMOS technology offers an advantage of double-side processing of the membrane before and after bonding, and since after bonding the top layer is the 200-nm thick n-InP, a DFB grating can be fabricated in this layer with a high coupling constant. The grating has a $\pi/2$ phase shift in the center. The light is coupled from the DFB region into the passive waveguide and then through the grating coupler (GC) into the single-mode fiber.

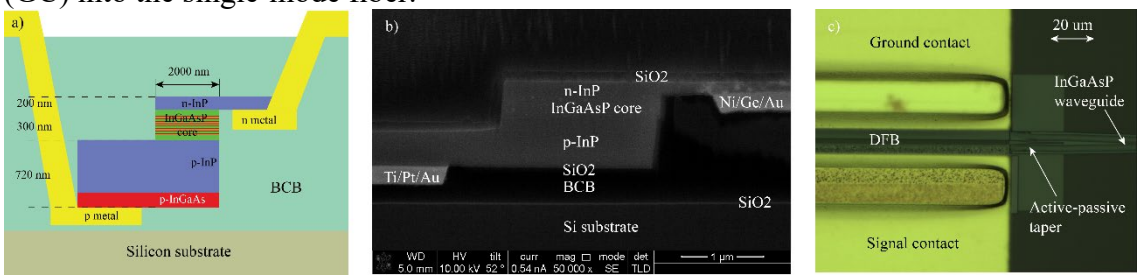

Figure 1. a) Schematic cross-section of the laser; b) FIB image of the cross-section; c) optical microscope image with the top view of the finished laser

Measurements

First, we measure the static characteristics of lasers. The full wafer was mounted on a copper chuck with temperature control by Peltier element. The GS contacts are probed with DC probe, the ILX current source is used for DC bias and the output optical signal is coupled through the GC into a vertical single mode fiber. Here, we present performance of a 250 µm long DFB which has a deeply etched grating. The grating coupling constant is fitted from the sub-threshold spectrum and equals ≈ 500 cm^{-1}. All measurements are done at 10 °C, since at higher temperatures the performance degrades significantly. On Figure 2a LIV curve of the laser is shown. The threshold current is around 10 mA. At the threshold, the lasing wavelength is in the center of the DFB stop-band, however at higher currents it hops to the mode located at the right flank of the stop-band due to spatial hole burning and self-heating, and stays there until the thermal roll-off. On Figure 2b, the laser spectrum is demonstrated. The lasing wavelength is 1536 nm. The ripples visible inside the DFB stop-band correspond to strong reflections from the GC, which will be discussed later.

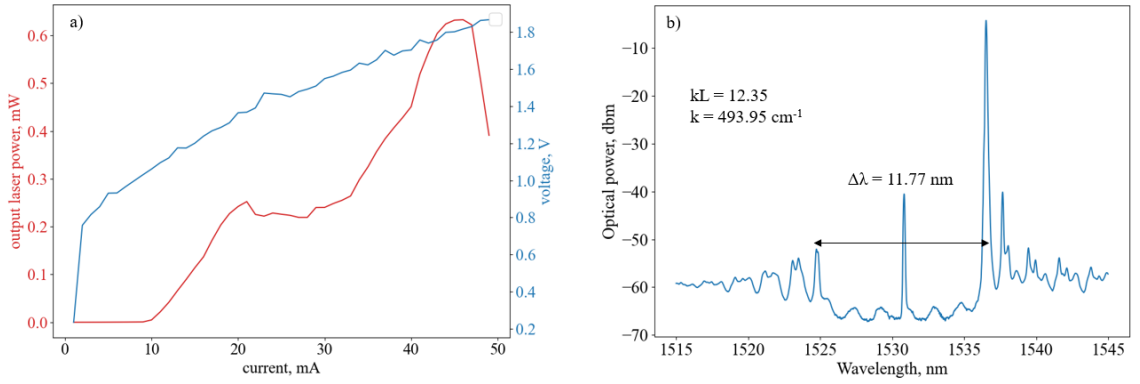

Figure 2. a) LIV curve of the laser at 10C. b) spectrum measured at 45 mA

The RF measurements are performed using the same wafer stage and coupling, however

we use a 40GHz GS probe and a bias T to supply both DC and AC current to the laser. Keysight N4373D Lightwave component analyzer is used to generate RF signal and measure electro-optical S parameters. Measured EO response is shown on Figure 3a. The highest measured bandwidth is 15 GHz at 40 mA.

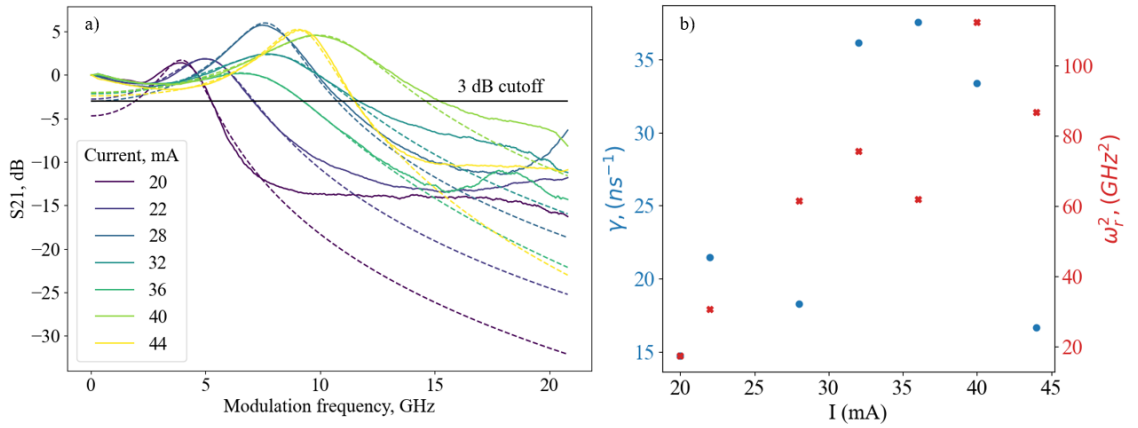

Figure 3. a) Small signal EO response measured with LCA (solid lines) and fit made using a 3-pole transfer function (dashed lines). b) Damping factor and relaxation oscillation frequency extracted from the fit

For the large signal analysis we use NRZ signal with pattern length $2^7 - 1$. The optical output of the laser is fed to the photodiode, and the output of the photodiode is connected back to the Multilane BER testing input. We obtain open eye diagrams for bitrates up to 25 Gbit/s with extinction ratio of 2.5 dB, without forward-error correction (FEC). Electro-optical eye diagrams and BER measured without EDFA at 25 Gbit/s are shown on Figure 4. We also used EDFA to amplify the signal and obtained BER of 1E-9, when the input power on the photodiode was 0 dBm.

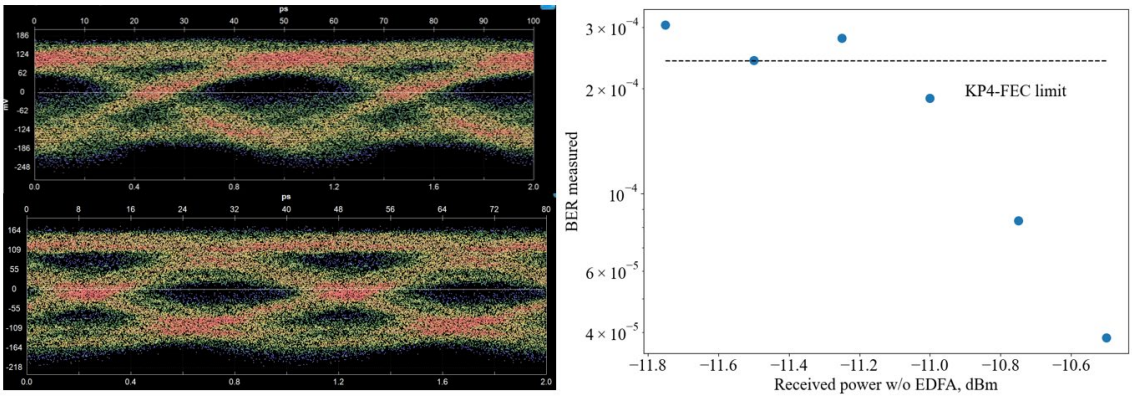

Figure 4. Left: eye diagrams for 20 and 25 Gbit/s NRZ signal. Right: BER measured at 25 Gbit/s with and without EDFA

Discussion

We fitted the sub-threshold laser spectrum to extract cavity parameters, influencing the laser performance and found a strong reflection from the GC (around 7%), which leads to mode hops. We also fitted the small-signal response with a 3-pole transfer function [8], and the fitted curves are shown on Figure 3a along with the measurement data. The 3-poles fit gives an information about ω_r, γ and RC limit, however for this laser, the measurements do not fit well with the model, which makes it difficult to extract the RC limit. The fit is only good at low frequencies and around the ω_r, and at high frequencies the measured S21 drops slower than what model predicts, which suggests, that other

modes contribute to the S21 (photon-photon resonance). A very suppressed second peak is visible in S21 around 20 GHz, however, the laser makes a mode hop before this peak is high enough to contribute to the laser bandwidth. We extract the damping factor γ, and plot its dependence on relaxation oscillation frequency square on Figure 3b. Normally, both γ and ω_r^2 should increase linearly with current, however in this laser it is not the case: at 40 mA, we observe drop of γ, while ω_r^2 reaches its maximum. This effect might be attributed to detuned loading, which happens due to reflections from the GC, however, in this laser it is weakly manifested. Since normally low reflections from the GC are desired for better laser stability, it might be necessary to introduce an extra reflector before the GC to provide a reflection for detuned loading and achieve a bandwidth extension.

Conclusion

We designed, fabricated and measured membrane DFB lasers with butt-joint coupling into the passive InGaAsP waveguide on IMOS platform. In particular, a 250 μm long DFB laser with a deeply etched DFB gives an output power of up to -2.5 dBm in the fiber, has a modulation bandwidth of 15 GHz and can be used for data transfer at 25 Gbit/s. The lasers were designed as a building block for integrated photonic platform and can be used in the future as part of more complex C-band optoelectronic transceivers, also interconnected with Si or InP electronics.

Acknowledgements

This work was supported by the Huawei research grant HDMI. The devices were fabricated using facilities of Nanolab @ TU/e.

References

[1] S. Yamaoka *et al.*, "Directly modulated membrane lasers with 108 GHz bandwidth on a high-thermal-conductivity silicon carbide substrate," *Nat. Photonics*, vol. 15, no. 1, pp. 28–35, Jan. 2021, doi: 10.1038/s41566-020-00700-y.

[2] S. Yamaoka *et al.*, "Uncooled 100-GBaud Directly Modulated Membrane Lasers on SiC Substrate," *J. Light. Technol.*, vol. 41, no. 11, pp. 3389–3396, Jun. 2023, doi: 10.1109/JLT.2023.3239614.

[3] Y. Matsui, R. Schatz, D. Che, F. Khan, M. Kwakernaak, and T. Sudo, "Low-chirp isolator-free 65-GHz-bandwidth directly modulated lasers," *Nat. Photonics*, vol. 15, no. 1, pp. 59–63, Jan. 2021, doi: 10.1038/s41566-020-00742-2.

[4] W. Yao *et al.*, "Towards the integration of InP photonics with silicon electronics: design and technology challenges," *J. Light. Technol.*, vol. 39, no. 4, pp. 999–1009, Feb. 2021, doi: 10.1109/JLT.2020.3043799.

[5] Y. Jiao *et al.*, "Indium Phosphide Membrane Nanophotonic Integrated Circuits on Silicon," *Phys. Status Solidi A*, vol. 217, no. 3, p. 1900606, 2020, doi: 10.1002/pssa.201900606.

[6] M. Spyropoulou *et al.*, "Towards 1.6T datacentre interconnect technologies: the TWILIGHT perspective," *J. Phys. Photonics*, vol. 2, no. 4, p. 041002, Jul. 2020, doi: 10.1088/2515-7647/ab9bf6.

[7] L. A. Coldren, S. W. Corzine, and M. L. Mašanović, *Diode Lasers and Photonic Integrated Circuits: Coldren/Diode Lasers 2E*. Hoboken, NJ, USA: John Wiley & Sons, Inc., 2012. doi: 10.1002/9781118148167.

[8] O. Kjebon, R. Schatz, S. Lourdudoss, S. Nilsson, and B. Stålnacke, "Modulation response measurements and evaluation of MQW InGaAsP lasers of various designs," presented at the SPIE, 1996, pp. 138–152. Accessed: Nov. 04, 2023. [Online]. Available: https://urn.kb.se/resolve?urn=urn:nbn:se:kth:diva-12522

[9] A. Zozulia *et al.*, "Design of InP membrane SOA with butt-joint active passive interface: 26th Annual Symposium of the IEEE Photonics Benelux Chapter," *IEEE Benelux Photonics Chapter Annu. Symp. 2022 24-25 Novemb. 2022 Eindh. Univ. Technol. Neth.*, 2022.